Molecular dynamics simulation of the transition from dispersed to solid phase

A. Chakrabarti, D. Fry,* and C.M. Sorensen
Department of Physics, Cardwell Hall, Kansas State University, Manhattan, Kansas 66506-2601, USA
(Received 16 July 2003; published 31 March 2004)

Molecular dynamics simulations in two dimensions of particles interacting with finite potentials comparable to k_BT yield aggregates which cross over from a fractal to a compact crystalline morphology. Growth kinetics and aggregate size distributions evolve from nonequilibrium to equilibrium limits.

DOI: 10.1103/PhysRevE.69.031408 PACS number(s): 82.70.Gg, 82.70.Rr

In a wide variety of natural and technical settings small particles in a dispersed phase come together to form larger clusters when the small particle system becomes, by some manner, unstable [1]. From a broad perspective, the ''particles'' can be atoms, ions, or molecules, as well as colloidal particles, and the transition from a dispersed phase to clusters can include the formation of precipitated crystalline solids from solutions as well as the formation of fractal aggregates in colloids and aerosols [1,2]. Formation of condensed, crystalline solids or open, random aggregates represent the equilibrium and nonequilibrium limits of this transition. Limiting nonequilibrium models exist [3] and are successful in describing aggregation: (i) diffusion limited cluster aggregation (DLCA) where the rate limiting step is the Brownian diffusion by which the particles meet and stick irreversibly, and (ii) reaction limited cluster aggregation (RLCA) where the limiting step is the small probability of cluster sticking when they touch. There is, however, no general theory that encompasses the entire dispersed state to solid transition.

In this letter we present molecular dynamics simulations which span the gap between the equilibrium and nonequilibrium limits. We demonstrate our general results with simulations of a specific example, a two-dimensional secondary minimum colloid [4], by comparing cluster morphology and kinetics to the traditional DLCA, RLCA [3] and aggregation-fragmentation models [5,6].

The interactions between two charged colloidal particles in a prototypical charge-stabilized colloidal solution (such as polystyrene spheres in water) can be described in terms of a screened electrostatic repulsion plus a van der Waals attraction, the DLVO potential [4]. In addition to the primary van der Waals minimum at contact, the superposition of these two interactions can also lead to the formation of a secondary minimum [4,8] in the interaction potential between two spheres. If the depth of this secondary minimum is a few k_BT and if it is separated from the primary van der Waals minimum by a large Coulomb barrier, aggregation will be controlled by this secondary minimum and hence will be reversible. In pioneering work Skjeltorp [9] studied *two-dimensional* aggregates of polystyrene spheres attracting via a strong (several k_BT) secondary minimum. Skjeltorp's clusters ranged from fractal aggregates with coordination ≈ 2 to aggregates with hexagonally-packed crystalline morphology on short length scales and a ramified fractal morphology on large scales, to dense, faceted crystals. Our simulations replicate much of this morphology as the secondary minimum depth is changed. They also show how growth kinetics and resulting cluster size distributions evolve from the DLCA and RLCA limits to systems which approach equilibrium due to fragmentation, which is readily allowed by a shallow minimum. Our results are quite general but have specific application to other diverse situations including protein crystallization [10], binary colloids on a substrate under the influence of an ac electric field [11], and colloids interacting via depletion forces [12,13]. An example of the latter is Hobbie's work [13] on depletion driven self-assembly of colloids in *two dimensions* that shows reversible aggregation and eventual crystallization. The equations of motion in the constant temperature molecular dynamics method used here read as

$$\ddot{\vec{r}}_i = -\vec{\nabla} U_i - \Gamma \dot{\vec{r}}_i + \vec{W}_i(t), \tag{1}$$

where Γ is the monomer friction coefficient and $\vec{W}_i(t)$, which describes the random force acting on each colloidal particle, is a Gaussian white noise with zero mean and satisfies the two dimensional fluctuation-dissipation relation $\langle \vec{W}_i(t) \cdot \vec{W}_j(t') \rangle = 4k_BT\Gamma \delta_{ij}\delta(t-t')$. Hydrodynamic interactions, including lubrication forces, are ignored in the simulation as they may not be of predominant importance for a study of quiescent secondary minimum colloids [7]. The potential U is modeled by the DLVO potential consisting of a screened electrostatic repulsion and a van der Waals attraction [8]:

$$U(x) = J_0 \frac{e^{-k(x-1)}}{x} - \frac{A}{12} h(x), \tag{2}$$

where $x = r/\sigma$ is the reduced distance between the centers of two particles with σ being the diameter of the particles, k is the reduced inverse Debye length, J_0 is the electrostatic coupling constant related to the surface or zeta potential, A is the Hamaker constant (considered to be 6.5×10^{-20} J for polystyrene spheres), and the function $h(x)$ describes the van der Waals attraction:

$$h(x) = \frac{1}{x^2-1} + \frac{1}{x^2} + 2 \ln\left(1 - \frac{1}{x^2}\right). \tag{3}$$

*Present address: Polymers Division, National Institute of Standards and Technology, Gaithersburg, MD 20899, USA.

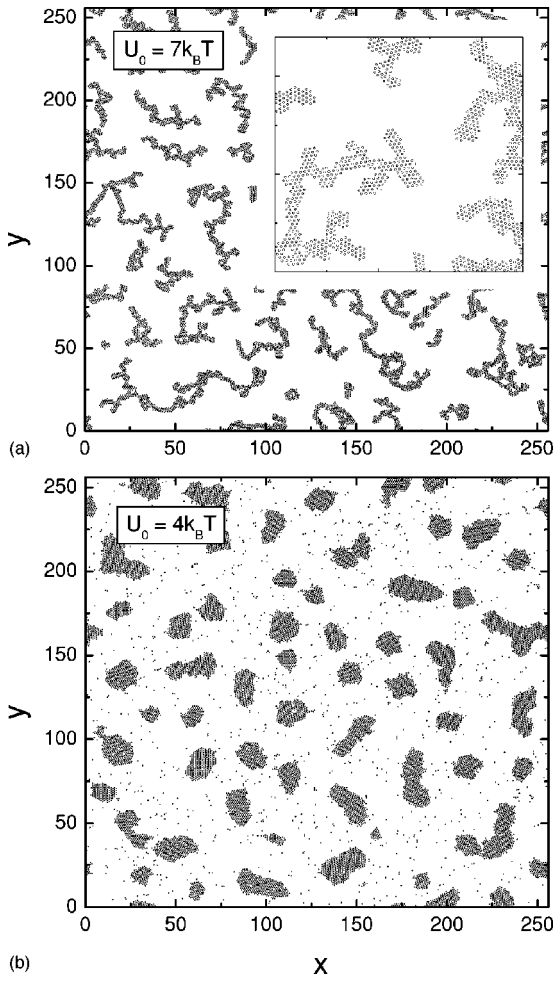

FIG. 1. Late time ($t=5000$) snapshots of the system for (a) $U_0=7k_BT$ and (b) $U_0=4k_BT$. The inset of (a) shows hexagonal closed-packed crystalline ordering at short length scales.

The parameters of the potential $U(x)$ are chosen such that there is a secondary minimum at $x=1.061$ with well depth U_0 and an energy barrier $>10k_BT$ at $x=1.01$. The potential is cut off at $x=1.5$. We have integrated [14] the equations of motion for a system size of 256^2 and 13 107 particles with $\Gamma=0.5$ and a time step $\Delta t=0.005$ in reduced units of $\sigma(m/J_0)^{1/2}$ with $m=1$. In Figs. Fig. 1(a) and 1(b) we show late-time snapshots for secondary well depth $U_0=7k_BT$ and $4k_BT$, respectively. A striking similarity to Skjeltorp's cluster morphology is seen in Fig. 1(a) for $U_0=7k_BT$: the aggregates show hexagonal closed-packed crystalline ordering at short length scales [inset of Fig. 1(a)] but ramified fractal nature at larger length scales. To be specific, this cluster morphology cannot be reproduced by a traditional DLCA modeling for which the typical coordination number of a particle in a cluster is ≈ 2. For a shallower well depth, $U_0=4k_BT$, the clusters are compact and the presence of a steady large number of monomers in the system at late times suggest a solid-gas equilibrium. The approach to equilibrium is quantified by the evolution of mean cluster size as we will present shortly.

The *large length scale* cluster morphology is quantified in Fig. 2 by showing the evolution of the fractal dimension of

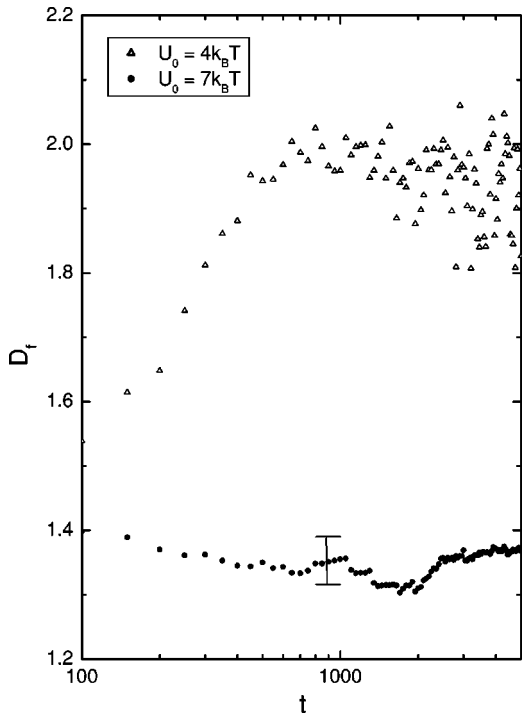

FIG. 2. Mass fractal dimension D_f as a function of time t.

an ensemble of clusters for both values of U_0 considered in the simulations. The fractal dimension of the clusters for $U_0=7k_BT$, determined from the slope of a log-log plot of radius of gyration versus number of particles for an ensemble of clusters, compares well with the accepted value ($D_f=1.4$) of the fractal dimension of two-dimensional (2D) DLCA clusters. It is truly remarkable that molecular dynamics (MD) simulations for a deep well depth, $U_0=7k_BT$, reproduce the same large-scale fractal dimension as in 2D DLCA, even though the short length scale structures of the clusters are totally different in these two models. In contrast MD simulations with a well depth of $U_o=4k_BT$ produce compact clusters with $D_f=2$ that, as shown below, are in equilibrium with a monomer gas.

For further quantitative comparison of the MD calculation with traditional models, we compute the mean-size of clusters s and the cluster-size distribution $n(N)$. For $U_0=7k_BT$, one would expect that fragmentation of clusters will be rare and a comparison with DLCA simulations will be meaningful over the simulation time [15]. For this reason, we also carry out large-scale DLCA calculations in two dimensions for a comparison with $U_0=7k_BT$ results. In Fig. 3(a) we show a log-log plot of the mean cluster size s versus time t. The kinetic exponent for the MD simulations is found to be $z=0.69\pm0.05$ while for the 2D DLCA [16] [as shown in the inset of Fig. Fig. 3(a)] $z=0.69\pm0.03$, clearly demonstrating that MD simulations do reproduce DLCA kinetics for deep enough well depths.

Although not a main focus of this study, it is still worthwhile to introduce a scaling argument to understand the value of the kinetic exponent z. We first note that the kinetic exponent z is related to the homogeneity of the aggregation kernel λ by $z=1/(1-\lambda)$. Next, we write the aggregation

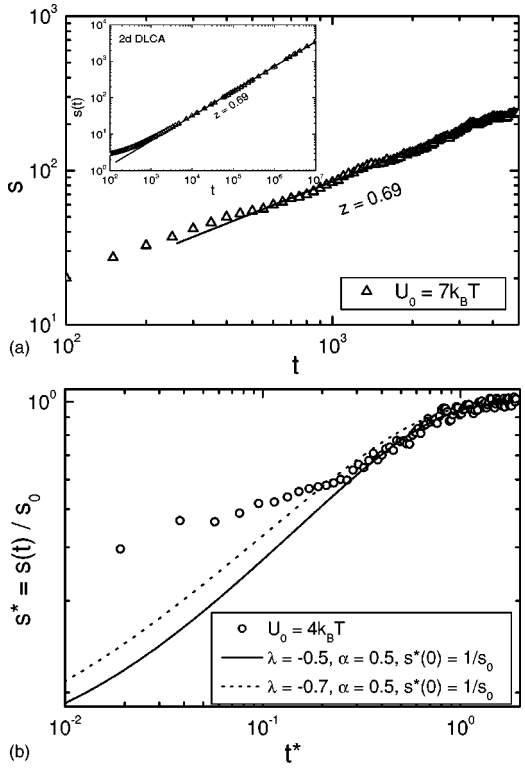

FIG. 3. (a) Log-log plot of mean size s as a function of time t for $U_0=7k_BT$ from 2D MD simulations. The inset shows results for 2D DLCA simulations. (b) Log-log plot of the reduced mean size s^* as a function of reduced time t^* for $U_0=4k_BT$. Results are compared with the theoretical result [6] for coagulation-fragmentation.

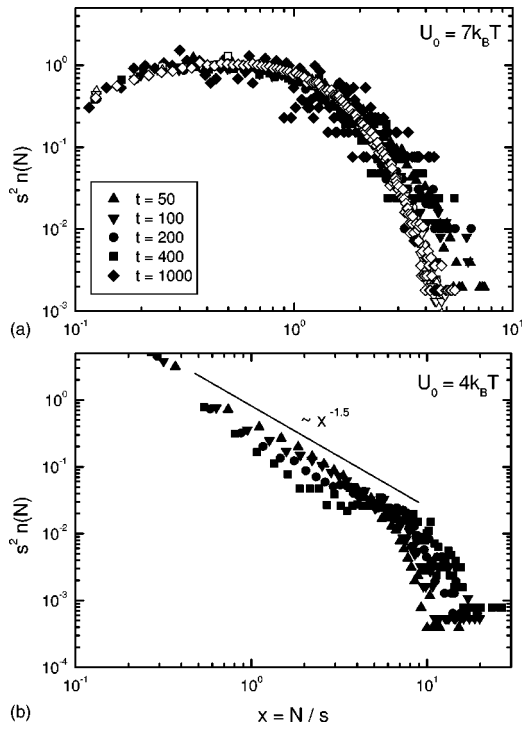

FIG. 4. Scaling of the cluster size distribution.The times are the same in both figures. The results are averaged over 10 runs. In (a), open symbols represent the scaled cluster-size distribution for a 2D DLCA simulation.

kernel K as a product of an area cross section $A=R^{d-1}$ and a characteristic velocity v, i.e., $K=vA$. Here, R is the mean radius of the clusters containing N particles. In the dilute limit, the characteristic velocity $v=D_0/R$ where D_0 is the diffusion constant. Since $D_0\sim 1/R$ for Brownian aggregation, we obtain $K\sim R^{d-3}$. Since, $N\sim R^{D_f}$,$K\sim N^{(d-3)/D_f}$. Thus, $\lambda=(d-3)/D_f$ in the dilute limit. In three dimensions, this provides $\lambda=0$ and $z=1$ as expected [2]. In two dimensions, however, $\lambda=-1/D_f=-0.7$ with $D_f=1.4$ and hence $z=0.59$ in the dilute limit. Since the clusters are fractals, the cluster volume fraction (f_v^c) increases as aggregation proceeds. It is known that the kinetic exponent z increases as the system gets dense [17]. In this cluster dense regime, one can understand this increase of z by considering that the characteristic velocity is now given by D_0/R_{nn} where R_{nn} is the nearest neighbor distance and scales as $R_{nn}\sim N_c^{1/d}$ where N_c is the number of clusters in the system. Since $NN_c=N_m$, the number of monomers in the system which is a constant, $K\sim N^{(d-2)/D_f-1/d}$ at the intermediate regime. This implies $\lambda=0.22$ in three dimensions with $D_f=1.8$ and hence $z=1.28$ as seen before [17]. In two dimensions, on the other hand, $\lambda=-0.5$ in this cluster dense regime yielding $z=0.67$ in good agreement with both the 2D DLCA simulation and MD calculations shown in Fig. Fig. 1(a).

The similarity between MD simulation for deep secondary well minimum and DLCA is further demonstrated in Fig. 4(a) where we plot the scaled cluster size distribution. This graph demonstrates that scaling works well for MD simulations and, more importantly, the scaled size distribution matches extremely well the distribution computed from the 2D DLCA simulation.

We now turn our attention to the MD results for a shallow well depth, namely, for $U_0=4k_BT$. In this case, the fragmentation of the clusters plays an important role and the number of clusters and the cluster size distribution approach a steady state at late times. A mean-field model of random bond fragmentation has been introduced by Family, Meakin, and Deutch [5] and by Sorensen, Zhang, and Taylor (SZT) [6] which compare well with simulations of coalescing and randomly fragmenting drops [18]. However, the validity of such mean-field models in the context of real, reversible aggregation is not known. Thus, a comparison of MD results with random-bond fragmentation models will be important.

In terms of reduced variables $s^*=s/s_0$ and $t^*=t/t_0$ SZT finds the following differential equation:

$$ds^*/dt=s^{*\lambda}-s^{*\alpha+2}, \tag{4}$$

where s_0 is the steady state mean size, t_0 is the time to reach the steady state, and α is the fragmentation kernel homogeneity. We numerically solve this first order differential equation for $\lambda=-0.7$ and -0.5, the two values of λ found in two dimensions in the dilute and cluster dense regimes. In the SZT model, fragmentation is assumed to take place randomly throughout the cluster, while here we expect cluster fragmentation to occur mostly at the surface. One can, how-

ever, choose $\alpha=1/2$ in the mean-field model of SZT to roughly incorporate this possibility. In Fig. 3(b) we show results for the MD simulation for $U_0=4k_BT$ along with the numerical results from Eq. (4). The results compare well at late times during the approach to equilibrium. The early-time MD data totally deviate from the mean-field results of SZT, and can be fit to a power-law which is reminiscent of an Ostwald ripening process [19].

A scaling of the cluster-size distribution for $U_0=4k_BT$ shows a RLCA type power-law behavior, indicating that for this shallower well depth clusters do not stick the first time they approach each other. Such a power-law form in the scaling distribution has been observed by Hobbie [13] in experiments with 2D depletion-driven colloids. There is also a hint of an exponential decay in the scaled size distribution for large x as seen by Hobbie.

In summary, we have carried out molecular dynamics simulations of two-dimensional secondary minimum colloids to obtain a broad perspective into the dispersed-phase to solid-phase transition. We find that the morphology evolves from a DLCA fractal morphology with increasing monomer coordination to compact crystals. The time at which this crossover occurs depends on the well depth. The aggregation kinetics and size distribution evolve from the DLCA limit to a situation similar to RLCA but with fragmentation that allows a steady state, equilibrium size to be obtained.

Financial support for this work was given by NASA Grant No. NAG 3-2360.

[1] *Kinetics of Aggregation and Gelation*, edited by F. Family and D. Landau (North-Holland, Amsterdam, 1984).
[2] S.K. Friedlander, *Smoke, Dust and Haze* (Oxford University Press, New York, 2000).
[3] P. Meakin, J. Sol-Gel Sci. Technol. **15**, 97 (1999).
[4] J. Israelachvili, *Intermolecular and Surface Forces* (Academic Press, San Diego, 1994).
[5] F. Family, P. Meakin, and J.M. Deutch, Phys. Rev. Lett. **57**, 727 (1986).
[6] C.M. Sorensen, H.X. Zhang, and T.W. Taylor, Phys. Rev. Lett. **59**, 363 (1987).
[7] N.Q. Nguyen and A.J.C. Ladd, Phys. Rev. E **66**, 046708 (2002); J.F. Brady, J. Chem. Phys. **99**, 567 (1993); D.O. Reese *et al.*, Phys. Rev. Lett. **85**, 5460 (2000).
[8] J.M. Victor and J.P. Hansen, J. Phys. (France) Lett. **45**, L-307 (1984).
[9] A.T. Skjeltorp, Phys. Rev. Lett. **58**, 1444 (1987).
[10] R. Piazza, J. Cryst. Growth **196**, 415 (1999).
[11] W.D. Ristenpart, I.A. Aksay, and D.A. Saville, Phys. Rev. Lett. **90**, 128303 (2003).
[12] P.N. Segrè, V. Prasad, A.B. Schofield, and D.A. Weitz, Phys. Rev. Lett. **86**, 6042 (2001).
[13] E.K. Hobbie, Phys. Rev. Lett. **81**, 3996 (1998).
[14] W.F. van Gunsteren and H.J.C. Berendsen, Mol. Phys. **45**, 637 (1982).
[15] Over a much longer time scale, the $U=7k_BT$ clusters should eventually cross over from a fractal morphology to a compact morphology.
[16] The MD vs DLCA comparison is carefully carried out for approximately the same cluster volume fraction f_c^v at the latest time since the kinetic exponent z increases as f_c^v increases and the system gets dense [17].
[17] D. Fry, T. Sintes, A. Chakrabarti, and C.M. Sorensen, Phys. Rev. Lett. **89**, 148301 (2002).
[18] T. Sintes, R. Toral, and A. Chakrabarti, Phys. Rev. A **46**, 2039 (1992).
[19] For a review, see, for example, A.J. Bray, Adv. Phys. **43**, 357 (1994).